

# Preparation of Microporous Membranes from Cation Exchange Membranes Prepared by the Paste Method

YUKIO MIZUTANI, KOSHI KUSUMOTO, MASAKATSU NISHIMURA, TOSHIHIKO NISHIMURA, and EIJI ASADA,  
*Tokuyama Soda Co., Ltd., Tokuyama-City, 745, Japan*

## Synopsis

A microporous membrane is prepared by treating the cation exchange membrane ( $\text{Fe}^{+++}$  form) with an  $\text{H}_2\text{O}_2$  aqueous solution. The cation exchange membrane is prepared by the paste method: the base membrane is prepared beforehand and then sulfonated. The preparative conditions of the base membrane were studied in connection with the characteristics of the resultant microporous membrane. Furthermore, the availability of the microporous membrane for ultrafiltration was studied by using an aqueous solution of a bovine hemoglobin.

## INTRODUCTION

We have already reported the preparation of the ion exchange membranes by the paste method.<sup>1,2</sup> A paste, mainly consisting of poly(vinyl chloride) (PVC) powder, styrene (St), divinylbenzene (DVB), and a polymerization initiator, is coated onto a reinforcing material, and the monomers are copolymerized to prepare the base membrane. Then an ion exchange membrane is prepared by introducing an ion exchange group onto the base membrane.

The treatment of the cation exchange membrane ( $\text{Fe}^{+++}$  form) with an  $\text{H}_2\text{O}_2$  aqueous solution results in a microporous membrane,<sup>3,4</sup> applicable for ultrafiltration.<sup>5</sup> However, no details of the preparation of the microporous membrane has been reported yet. Accordingly, we studied some detailed relation between the preparative conditions of the base membrane and the properties of the resultant microporous membrane and also the applicability of the microporous membrane for ultrafiltration.

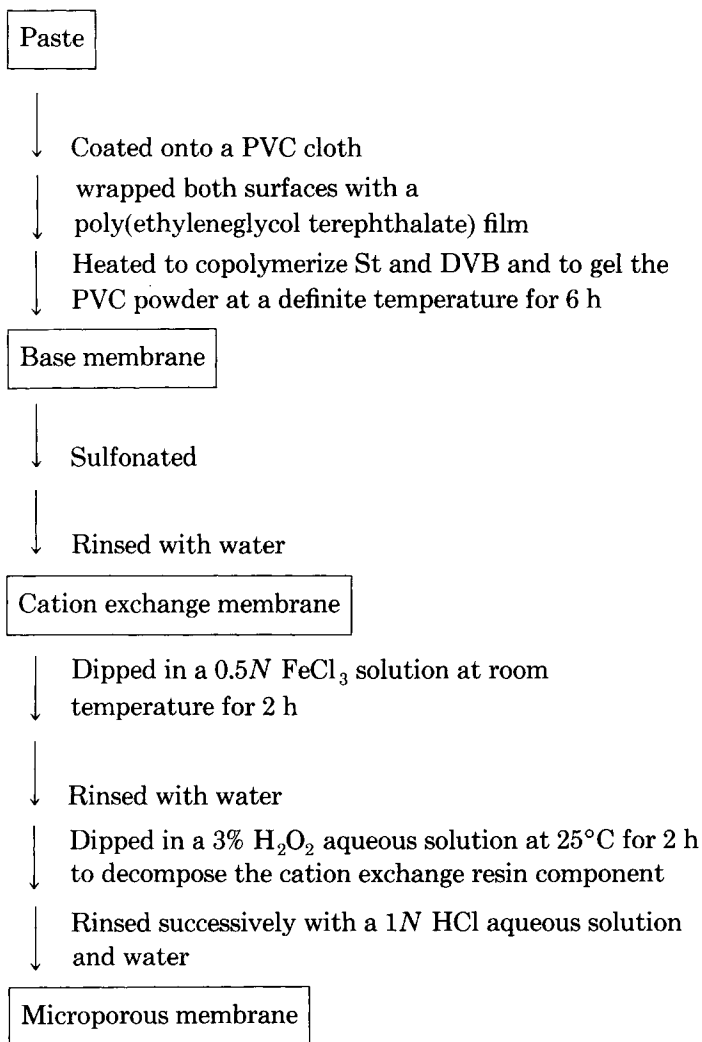
## EXPERIMENTAL

### Materials

All the materials used were of commercial grade. The content of the pure DVB isomers in the commercial DVB was 53% and the DVB quantity in this paper was shown as that of the commercial DVB. The polymerization initiators used were benzoylperoxide (BPO), *t*-butylperoxylaurate (PBL), and *t*-butylperoxybenzoate (PBZ).

### Preparation of Microporous Membrane

The preparative procedure is shown as follows. The cation exchange membrane was prepared by the paste method.<sup>1,2</sup> The paste was prepared by mixing PVC powder, St, DVB, dioctylphthalate (DOP), and a polymerization initiator.



The standard composition of the paste was as follows by weight if otherwise not noted: DOP/(St + DVB) = 0.2, DVB/(St + DVB) = 0.1, polymerization initiator/(St + DVB) = 0.01, and (St + DVB)/PVC = 6. The DVB/(St + DVB) and (St + DVB)/PVC ratios were varied in the range of 0–0.3 and 2–6, respectively.

### Water Permeability Measurement

The measurement was carried out at room temperature by the method shown in the previous paper.<sup>5</sup> The apparatus was similar to that used by Kopeček et al.<sup>6</sup> It was confirmed beforehand that the water permeation rate linearly increased with the increase in the applied pressure in the range of 0–8 kg/cm<sup>2</sup>, as reported in the previous paper.<sup>5</sup> The water permeability was determined from the slope of the linear relation.

### Determination of Apparent Pore Size, Pore Number, and Tortuosity Factor

The pore radius  $r$  (cm) and the pore number  $n$  (cm<sup>-2</sup>) can be calculated by using Poiseuille's law, as described in the previous studies, assuming that the pore is cylindrical and perpendicular to the membrane surface<sup>3,4,7</sup>:

$$K_p = \frac{\eta L Q}{A \Delta P} \quad (1)$$

$$r = \sqrt{(8/\epsilon) K_p} \quad (2)$$

$$n = \frac{\epsilon^2}{8\pi K_p} \quad (3)$$

$$\epsilon = \frac{W_e - W_d}{A L \rho_w} = \pi r^2 n \quad (4)$$

where  $Q$  is the water permeation rate (cm<sup>3</sup>/s),  $K_p$ , the specific permeability (cm<sup>2</sup>),  $\Delta P$ , the pressure difference across the membrane (dyn/cm<sup>2</sup>),  $W_e$ , the wet weight of the membrane (g),  $W_d$ , the dry weight of the membrane (g),  $A$ , the effective membrane area (cm<sup>2</sup>),  $L$ , membrane thickness (cm),  $\rho_w$ , density of water (g/cm<sup>3</sup>),  $\epsilon$ , porosity, and  $\eta$ , viscosity of water (poise).

The tortuosity factor ( $\sigma$ ) of the pore is defined as follows:

$$\sigma = R_m/R_i \quad (5)$$

$$R_i = R_n L/\epsilon \quad (6)$$

where  $R_m$  is the electric resistance of the microporous membrane in a 0.5N NaCl aqueous solution ( $\Omega$  cm<sup>2</sup>) and  $R_n$ , the specific electric resistance of the 0.5N NaCl aqueous solution ( $\Omega$  cm), measured at 25°C under an alternating current (1 kHz).<sup>8</sup>

### Ultrafiltration of Hemoglobin Solution

A bovine hemoglobin solution (1000 ppm and MW 6600–6800) was used for the test. The rejection of hemoglobin was defined as follows:

$$R_s (\%) = (1 - C_i/C_b) \times 100 \quad (7)$$

where  $C_f$  is the hemoglobin concentration of the filtrate and  $C_b$  is the concentration of the bulk solution. The hemoglobin concentration was determined by absorbance analysis at 410 nm.

The permeating cell, the reservoir of the hemoglobin solution (3 L), and the pipe line were made of stainless steel. The solution was circulated between the permeating cell and the reservoir with the aid of a pump. The circular membrane (effective area, 6.15 cm<sup>2</sup>) was placed on a porous support of the cell. The width of the solution path above the membrane was 5 mm. The solution inlet (inner diameter, 4 mm) was attached, vertically to the membrane surface, at the place near the periphery of the space above the membrane and the outlet (inner diameter, 4 mm) was similarly attached on the opposite place. The pressure of the solution was controlled by a pressure-controlling bulb, using a high-pressure nitrogen bomb. The time-dependent changes in the permeating rate and the rejection were measured.

## RESULTS AND DISCUSSION

In process of preparing the base membrane, the following reactions proceed simultaneously: the formation of the PVC gel phase from the PVC particles swollen with the monomer mixture and the phase-separating copolymerization of St-DVB in the PVC gel phase, engendered by the decomposition of the polymerization initiator. St and DVB are soluble in PVC but poly-St is not compatible with PVC, so that the resultant copolymer necessarily separates out of the PVC gel phase; furthermore, DVB promotes the phase separation. Accordingly, the resultant St-DVB copolymer is finely dispersed in the PVC gel phase, grafting onto PVC and intertwining with PVC. The St-DVB copolymer is sulfonated and then the resultant cation exchange resin component (Fe<sup>+++</sup> form) is selectively decomposed by treating with an H<sub>2</sub>O<sub>2</sub> aqueous solution to obtain the microporous membrane.<sup>3,4</sup> Therefore, the structure of the microporous membrane is dependent mainly on the morphology of the base membrane. Here, the swelling of the St-DVB resin component by sulfonation and the presence of DOP could not be taken into consideration owing to the insolvable complexity.

The water permeability of the microporous membrane is one of the most fundamental properties and then the effects of some conditions to prepare the base membrane on the water permeability were studied at first. Figure 1 shows the effect of the DVB/(St + DVB) ratio of the paste on the water permeability. When the DVB/(St + DVB) ratios were 0.2 and 0.3, the cation exchange resin component could not easily be decomposed under the standard condition (at 25°C for 2 h): the cation exchange membrane was treated with the H<sub>2</sub>O<sub>2</sub> aqueous solution at 25°C for 16 h. When the DVB/(St + DVB) ratio was 0.1, the water permeability was largest. The reason is obscure, but this result is consistent with that in the case of the preparation of the microporous membrane by copolymerizing St-DVB in a PVC film and decomposing the cation exchange resin component resulted by sulfonation of the copolymer.<sup>9</sup> So, the DVB/(St + DVB) ratio was fixed to be 0.1 in the subsequent study. Also, it was observed that the base membrane became more transparent with increasing the DVB/(St + DVB) ratio. The much more

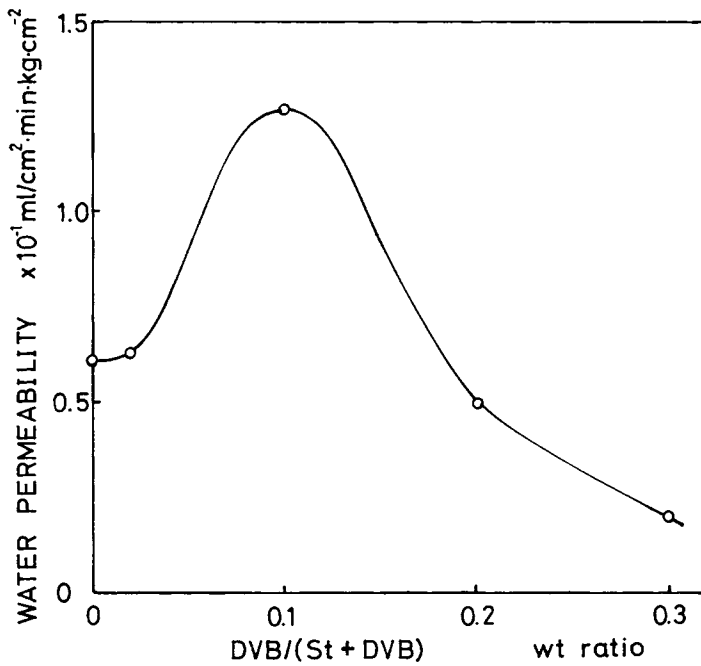


Fig. 1. The effect of the DVB/(St + DVB) ratio of the paste onto the water permeability of the microporous membrane. The composition of the paste except the DVB/(St + DVB) ratio was the standard one, using BPO. Copolymerization temperature 105°C.

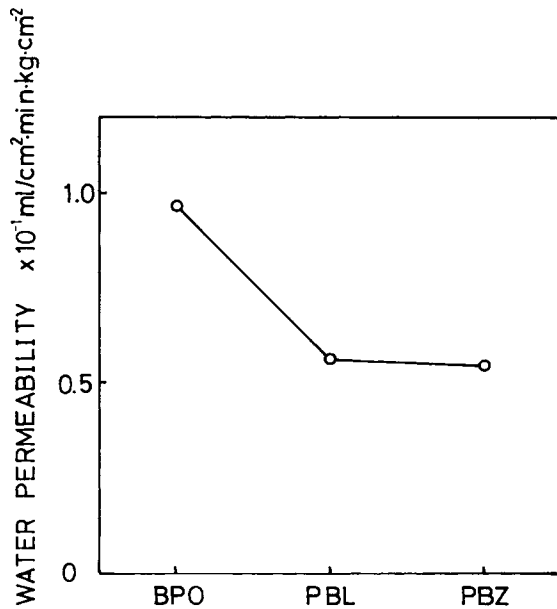


Fig. 2. The effect of the polymerization initiator onto the water permeability of the microporous membrane. The composition of the paste was the standard one. Copolymerization temperature 105°C.

DVB is used, the earlier the propagating St-DVB copolymer separates out and the more finely the resultant copolymer is dispersed in the PVC gel phase.

Figure 2 shows the water permeability when the various polymerization initiators were used. The order of their decomposability at 105°C is as follows: BPO > PBL > PBZ.<sup>10</sup> The morphology of the base membrane is determined by the competitive balance between the gellation rate of the PVC particles swollen with the monomer mixture and the copolymerization rate of St-DVB, engendered by the decomposition of the polymerization initiator. The more rapidly the initiator decomposes, the more rapidly the copolymerization proceeds. Therefore, the decomposability affects the balance between the competitive reaction rates described above. In the case of BPO, the water permeability was largest. Namely, it is reasonable that since the decomposition of BPO is more rapid, the copolymerization of St-DVB is more rapid. Accordingly, the copolymerization should proceed in the less gelled PVC phase in comparison with the other cases and the distribution of the resultant St-DVB copolymer in the base membrane should become rather coarse. This

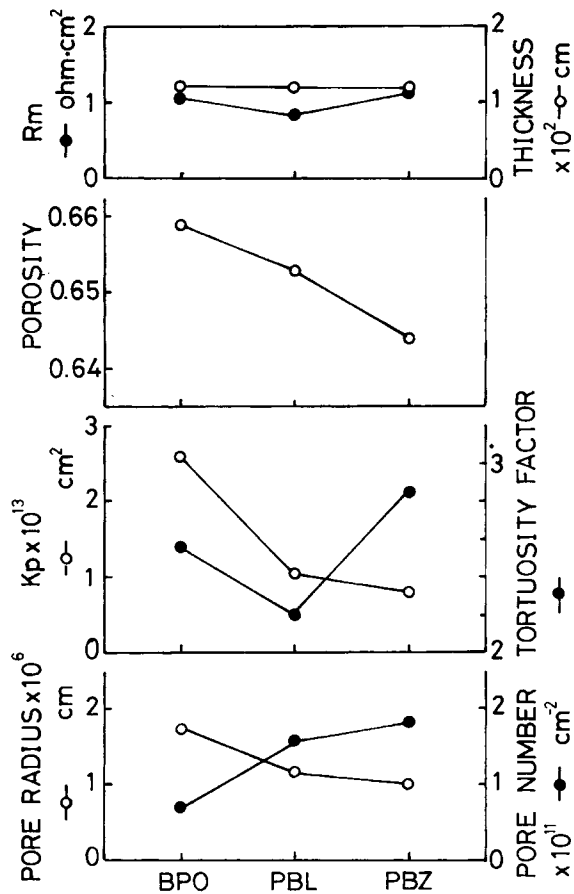


Fig. 3. The effect of the polymerization initiator onto the properties of the microporous membrane. The composition of the paste was the standard one. Copolymerization temperature 105°C.

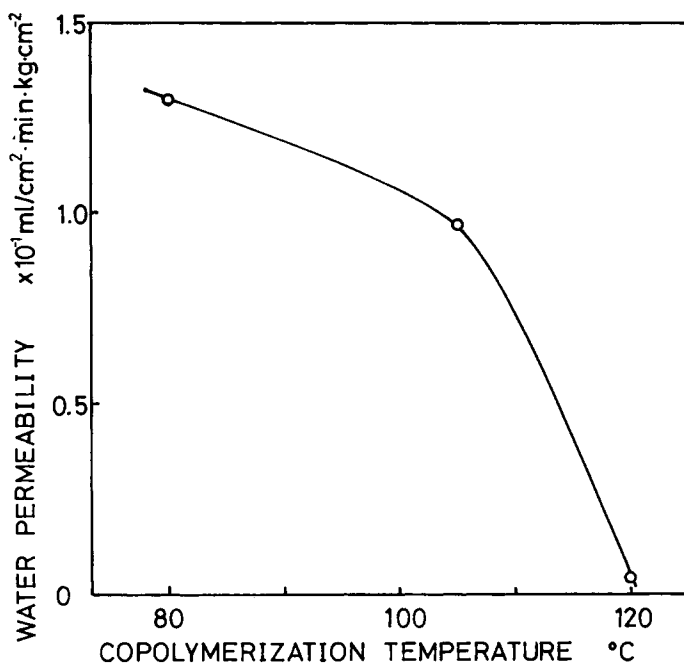


Fig. 4. The effect of the copolymerization temperature onto the water permeability of the microporous membrane. The composition of the paste was the standard one, using BPO.

should be the reason why the water permeability was largest in the case of BPO. The foregoing explanation is supported by the results shown in Figure 3. The pore radius, the porosity, and the  $K_p$  value in the case of BPO are larger than those in the other cases. It is interesting that the tortuosity factor in the case of PBL is smallest, although the porosity is between those in the case of BPO and PBZ, but its reason is inexplicable.

Figure 4 shows the relation between the water permeability and the copolymerization temperature. The higher the temperature, the smaller the water permeability. At the higher temperature, the gellation of the PVC particles more rapidly proceeds to result in the more gelled PVC phase and also BPO more rapidly decomposes. This means that more radicals generate in the more gelled PVC phase. Therefore, more copolymer radicals propagate and separate earlier out of the PVC gel phase. Then the resultant St-DVB copolymer is more finely dispersed in the PVC gel phase and therefore the water permeability of the microporous membrane becomes smaller. This explanation is supported by the results shown in Figure 5, which clearly shows the effect of the copolymerization temperature onto the characteristics of the microporous membrane. With increasing the temperature, the porosity, the pore radius, and the  $K_p$  value decrease and, contrarily, the pore number and tortuosity factor increase.

Figure 6 shows the effect of the (St + DVB)/PVC ratio of the paste onto the properties of the microporous membrane. It is necessary to note that the (St + DVB)/PVC ratio is the value of the paste, but not of the base membrane, because the paste is coated onto the PVC cloth and the monomers inevitably migrate into the PVC cloth.<sup>11</sup> For reference, when the

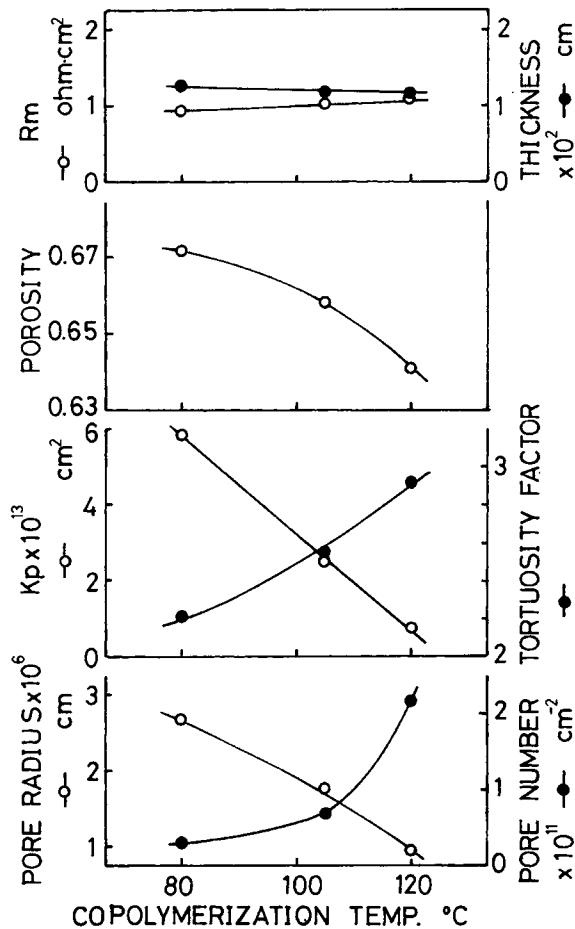


Fig. 5. The effect of the copolymerization temperature onto the properties of the microporous membrane. The composition of the paste was the standard one, using BPO.

(St + DVB)/PVC ratios are 6 and 2, the cation exchange capacities are 2.3–2.4 and 1.9–2.0 meq/g dry membrane, respectively. It is reasonable that the larger the (St + DVB)/PVC ratio, the larger the  $K_p$  value, the porosity, and the pore radius and, contrarily, the less the pore number and the tortuosity factor.

The effects of the preparative conditions of the base membrane shown in Figures 3, 5, and 6 are summarized in Table I. Regarding the polymerization initiator, the copolymerization temperature, and the (St + DVB)/PVC ratio, the orders of the  $K_p$ ,  $r$ , and  $\epsilon$  values are the same and those of the  $n$  and  $\sigma$  values are reversed except that of the  $\sigma$  value regarding the polymerization initiator.

Figure 7 shows the scanning electron microphotographs of the microporous membrane surfaces, relating to the effect of the DVB/(St + DVB) ratio of the paste. The relatively larger and smaller pores coexist in the rather continuous PVC phase, showing that the PVC particles gelled enough. Furthermore, the pores show the delicate distribution which should affect the membrane properties. When the DVB/(St + DVB) ratio is 0 and 0.02, the pore is larger.



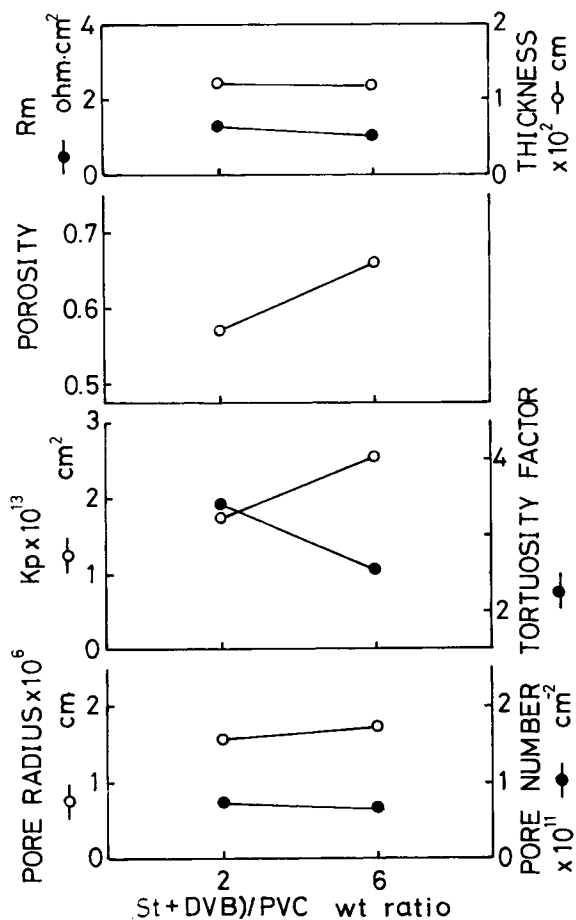


Fig. 6. The effect of the (St + DVB)/PVC ratio of the paste onto the properties of the microporous membrane. The composition of the paste except the (St + DVB)/PVC was the standard one, using BPO. Copolymerization temperature 105°C.

TABLE I  
Tendencies in the Effects of the Preparative Conditions onto the Characteristics of the Microporous Membranes

Polymerization initiator	Copolymerization temperature (°C)	(St + DVB)/PVC (wt ratio)
$K_p$ BPO > PBL > PBZ	80 > 105 > 120	6 > 2
$r$ BPO > PBL > PBZ	80 > 105 > 120	6 > 2
$n$ PBZ > PBL > BPO	120 > 105 > 80	2 > 6
$\epsilon$ BPO > PBL > PBZ	80 > 105 > 120	6 > 2
$\sigma$ PBZ > BPO > PBL	120 > 105 > 80	2 > 6

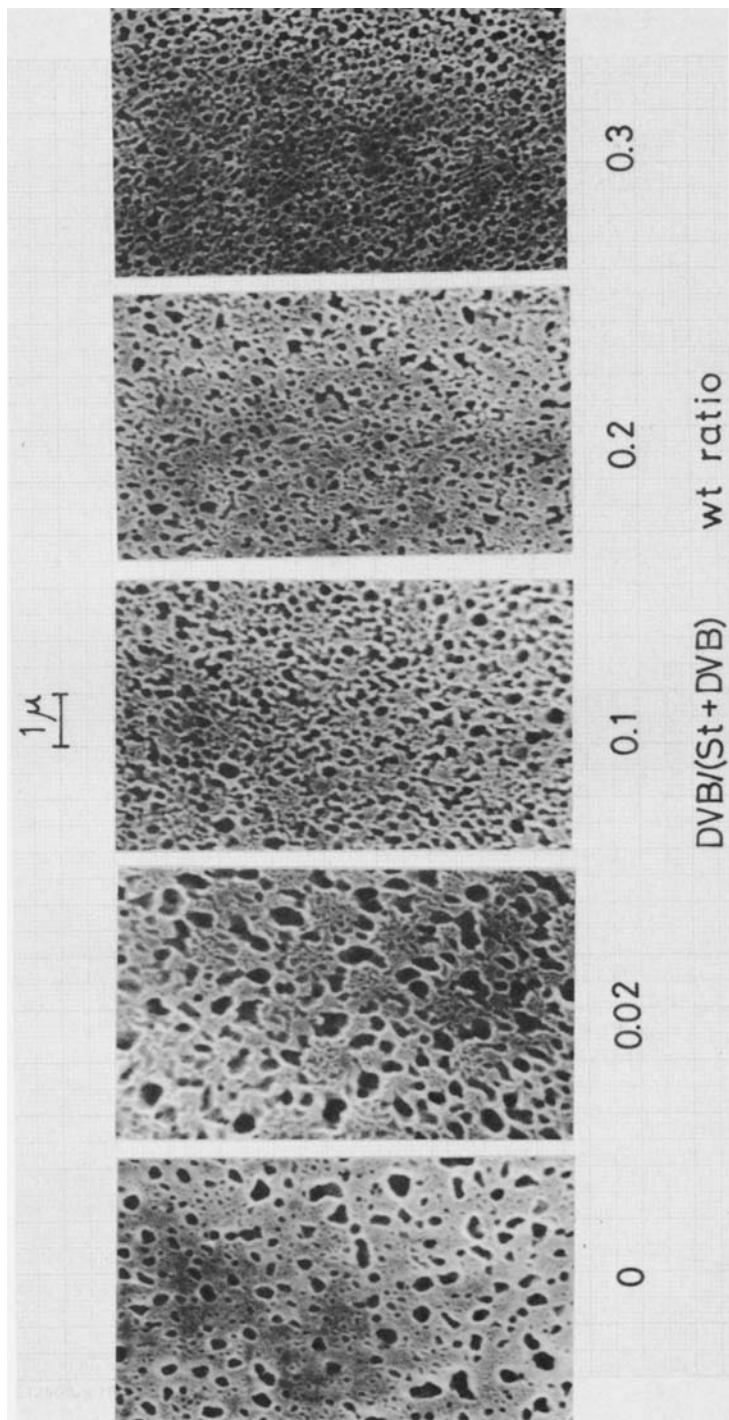


Fig. 7. The scanning electron microphotograph of the surface of the microporous membrane, relating to the effect of the DVB/(St + DVB) ratio of the paste. The conditions to prepare the membrane were the same as those shown in Figure 1.

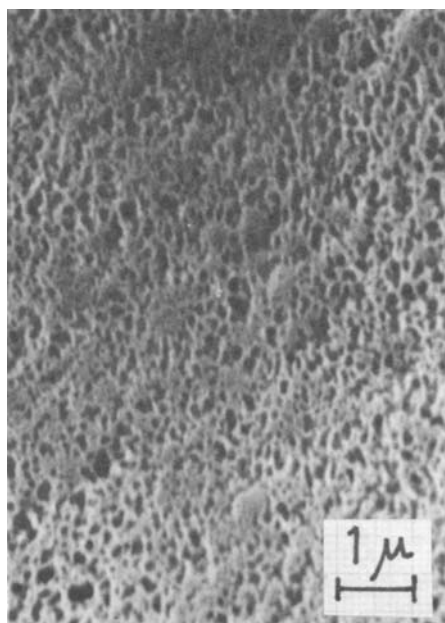


Fig. 8. The scanning electron microphotograph of the surface of the microporous membrane, prepared from the base membrane copolymerized at 80°C.

When the DVB/(St + DVB) ratio is 0.1, 0.2, and 0.3, the difference in the distribution of the pore size and number is slight, although the size of the larger pore seems to decrease with increasing DVB/(St + DVB). Figure 8 shows the surface of the microporous membrane, prepared from the base membrane copolymerized at 80°C. The membrane surface is rather coarse, showing that the copolymerization proceeds in the PVC phase not gelled enough. When the copolymerization temperature is  $> 105^{\circ}\text{C}$ , the membrane surface is continuous as shown in Figure 7. The difference in the continuity of the PVC phase supports the results shown in Figure 5. Figure 9 shows the surface of the microporous membrane, prepared from the base membrane copolymerized by using PBZ. The pore is evidently smaller than that in the case of BPO as shown in Figure 7 [DVB/(St + DVB) = 0.1]. Since PBZ is less decomposable than BPO, the copolymerization proceeds more slowly in the more gelled PVC phase and the resultant St-DVB copolymer is finely dispersed. Accordingly, the pore size reasonably becomes smaller. This supports the results shown in Figure 3.

Figures 10 and 11 show the effects of the applying pressure and the flow rate of the hemoglobin solution onto the rejection of hemoglobin and the water permeating rate, respectively, relating to the volume of the permeated water. The permeating rate gradually decreased at first and then leveled off. On the other hand, when the applying pressure was 5 kg/cm<sup>2</sup>, the rejection of hemoglobin decreased at first and then gradually increased. When the applying pressure was 3 and 8 kg/cm<sup>2</sup>, the rejection of hemoglobin decreased at first and then leveled off. The orders of the flow rates of the hemoglobin solution to enhance the rejection and the permeating rate were 0.4 L/

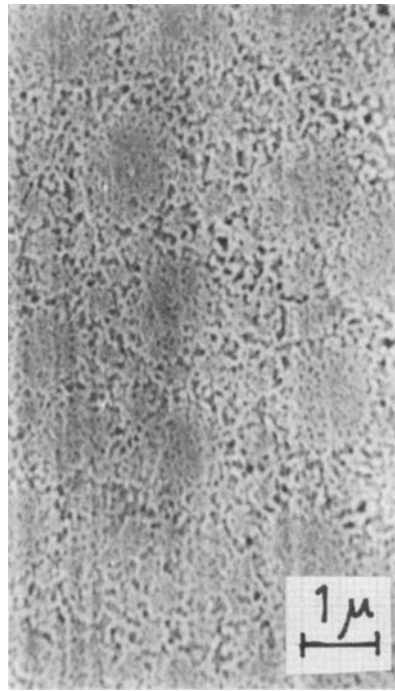


Fig. 9. The scanning electron microphotograph of the surface of the microporous membrane, prepared from the base membrane copolymerized at 105°C by using PBZ.

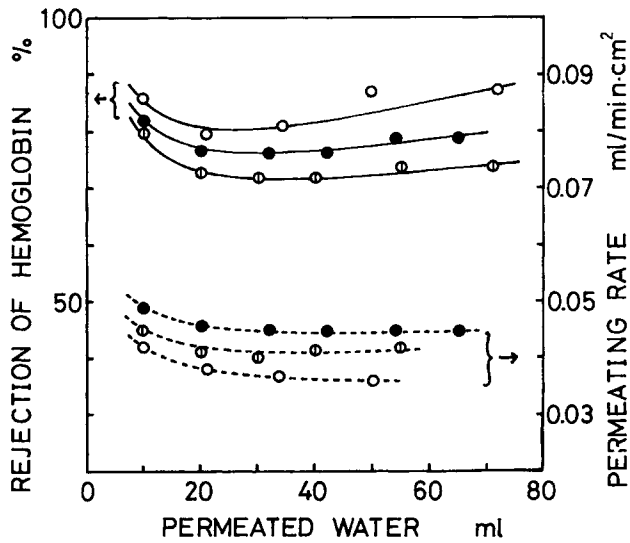


Fig. 10. The change in the rejection of hemoglobin and the permeating rate with increasing the permeated water volume, relating to the effect of the flow rate of the hemoglobin solution. The base membrane was prepared at 120°C by using BPO. Flow rate (L/min): (○) 0.4; (●) 1.0; (⊙) 1.6. Applying pressure 5 kg/cm<sup>2</sup>.

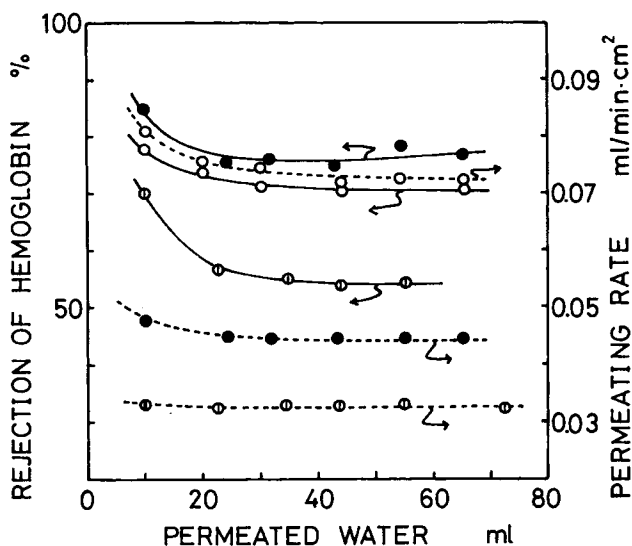


Fig. 11. The change in the rejection of hemoglobin and the permeating rate with increasing the permeated water volume, relating to the effect of the applying pressure. The membrane was the same as that shown in Figure 9. Applying pressure ( $\text{kg}/\text{cm}^2$ ): (○) 3; (●) 5; (○) 8. Flow rate 1.6 L/min.

min > 1.0 L/min > 1.6 L/min and 1.0 L/min > 1.6 L/min > 0.4 L/min, respectively. On the other hand, the orders of the applying pressure to enhance the rejection and the permeating rates were  $5 \text{ kg}/\text{cm}^2 > 8 \text{ kg}/\text{cm}^2 > 3 \text{ kg}/\text{cm}^2$  and  $8 \text{ kg}/\text{cm}^2 > 5 \text{ kg}/\text{cm}^2 > 3 \text{ kg}/\text{cm}^2$ , respectively. These results do not show any definite tendencies between the orders regarding the permeating rate and the rejection, suggesting that there should be a delicate optimum condition to ultrafiltrate the hemoglobin solution. Absence of the definite tendencies as described above and the gradual increase in the rejection after the decrease at the earlier stage should be ascribed to the deposition of hemoglobin onto the membrane surface and the membrane compaction.

As described above, the mechanism of the morphology formation in the base membrane and the formation of the micropore by the decomposition of the sulfonated resin component are still too complex to elucidate explicitly. Here, it is noteworthy that both the use of DOP and the formation of the graft copolymer of St-DVB onto PVC<sup>12,13</sup> should participate complicatedly in the pore formation, but these were not taken into consideration. Also, the results in this study are meaningful in understanding morphology of the polymer composite, resulted from the copolymerization of St-DVB in the PVC gel phase, as an example of a crosslinking phase-separation copolymerization in a polymer gel phase.

## References

1. Y. Mizutani, R. Yamane, H. Ihara, and H. Motomura, *Bull. Chem. Soc. Jpn.*, **36**, 361 (1963).
2. Y. Mizutani, R. Yamane, and H. Motomura, *Bull. Chem. Soc. Jpn.*, **38**, 689 (1965).
3. Y. Mizutani, *Bull. Chem. Soc. Jpn.*, **43**, 595 (1970).
4. Y. Mizutani and M. Nishimura, *J. Appl. Polym. Sci.*, **14**, 1847 (1970).

5. Y. Mizutani and M. Nishimura, *J. Appl. Polym. Sci.*, **25**, 2273 (1980).
6. J. Kopeček and S. Sourirajan, *Ind. Eng. Chem. Process. Des. Dev.*, **9**, 5 (1970).
7. S. Sanada, *J. Chem. Soc. Jpn. Ind. Chem. Sect. (Kōgyō Kagaku Zasshi)*, **42**, 625 (1939).
8. M. Nishimura and Y. Mizutani, *J. Appl. Electrochem.*, **11**, 165 (1981).
9. Y. Mizutani, K. Kusumoto, M. Nishimura, and E. Asada, unpublished.
10. *Organic Peroxides*, 9th ed., Japan Oil and Fat Co., Tokyo, 1982.
11. Y. Mizutani and M. Nishimura, *J. Appl. Polym. Sci.*, **25**, 2925 (1980).
12. Y. Mizutani, *J. Chem. Soc. Jpn. Ind. Chem. Sect. (Kōgyō Kagaku Zasshi)*, **65**, 1124 (1962).
13. Y. Kagiya, K. Shikata, and Y. Mizutani, *J. Appl. Polym. Sci.*, **23**, 1309 (1979).

Received January 30, 1989

Accepted February 7, 1989